Design and powering impact on ships by alternative marine energy carriers to determine the total environmental impact

This paper is part of the graduation project 'Alternative marine energy carrier impact on ship powering and the environment'

A.M. Snaathorst

Delft University of Technology

TU Delft

Design and powering impact on ships by alternative marine energy carriers to determine the total environmental impact

A.M. Snaathorst[1] and J.F.J. Pruyn[1]

[1] *Maritime and Transport Technology, TU Delft, The Netherlands*

Abstract

This paper investigates the spatial requirements of methanol, LNG, liquid hydrogen, ammonia, and batteries and their impact on ship design and powering for constant operational requirements. A parametric design tool for bulk carriers, tankers, and container ships has been developed for the energy carriers to determine the main engine brake power increase. The results indicate that all ship type and alternative marine energy carrier combinations require a higher total engine power and consequently a higher energy carrier consumption w.r.t. fuel oil. The resulting powering impact by methanol, LNG, and ammonia are limited, but liquid hydrogen and batteries show average total powering increases of 8% and 220%. The results are intended to determine the total environmental impact of the energy carriers including the consequent increased energy consumption.

Keywords: Ship design, Powering impact, Alternative marine energy carriers, Environmental impact.

1 Introduction

The maritime industry is responsible for 3% of the annual global CO_2 emissions which is a cause of global warming and the consequent climate change (IPCC 2021). The CO_2 emissions are formed during the combustion of fossil fuel oil (e.g. HFO) in ships for powering. Due to the fossil fuel market dominance there is an unsustainable technology lock-in and therefore a voluntary switch to a less harmful energy carrier is unlikely Vergragt, Markusson, and Karlsson 2011. However, in 2023 the new Carbon Intensity Indicator (CII) regulation by the International Maritime Organization (IMO) will go into effect for all commercials vessels (Bureau Veritas 2021). This regulation limits greenhouse gas (GHG) emissions by ships and it becomes stricter over time. The GHG strategy by the IMO aims to reduce GHG emissions by 50% by the year 2050 and completely eliminated before the end of this century (DNV-GL 2019b). Accordingly, fuel oil will be forced out of the ship powering market for what are now considered alternative marine energy carriers (AMECs).

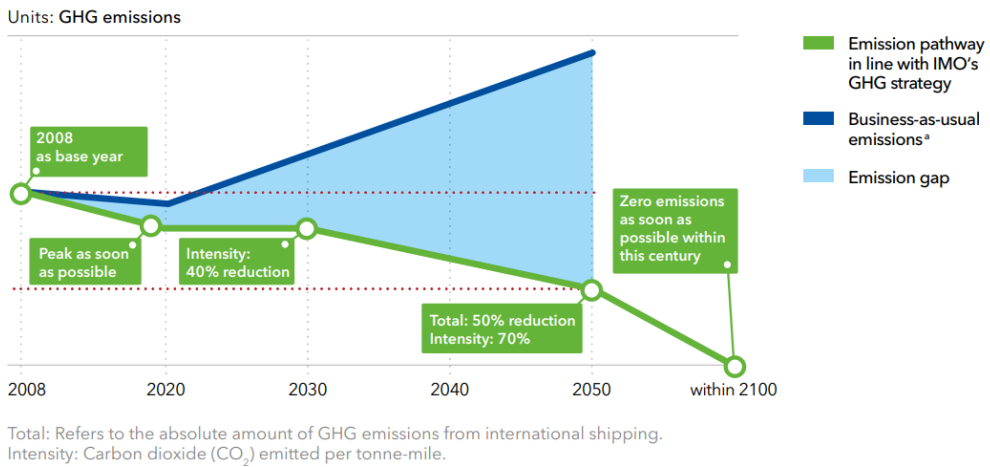

Figure 1. IMO's Initial Strategy GHG emission pathway (DNV-GL 2019b)

Liu and Duru (2019) compiled five different projections by various institutions on the outlook of marine energy carriers in 2050. The various outlooks still predict the presence of fossil fuel oil in 2050, but it is quickly making way for LNG, hydrogen based fuels, alcohol fuels, batteries, and bio/renewable versions of these energy carriers. Additionally, new powering technologies are accompanied by the AMECs, such as fuel cells and full electric power plants. However, all these AMECs have a lower contained volumetric and gravimetric energy density compared to fuel oil (DNV-GL 2019a). The shift from uncontained to contained energy density includes the storage tank and necessary systems. As a result, ship designs would require more volume and weight to accommodate the same amount of effective energy to perform the same operational requirements. In general, a larger and heavier ship results in higher propulsion powering and thus a higher energy carrier consumption.

It is generally acknowledged that the use of AMECs for equal power is more environmentally friendly. However, to the authors' knowledge, it has not been researched if this is still the case when taking the increased energy carrier consumption into account for constant operational requirements. In studies on AMECs, for example by Terün, Kana, and Dekker 2022 for new ultra large container ships and by Bodewes 2020 for a refit of a general cargo vessel, the cargo volume is surrendered, or the service speed and/or range are reduced to accommodate the additional bunker space. This paper investigates the impact of AMECs on ship designs and powering to support determining the total environmental impact. This is achieved by adding overall internal volume to existing ship designs through a parametric design tool to accommodate the additional AMEC bunker space.

2 Case study

The design and powering impact assessment consists of applying the spatial requirements for methanol, LNG, liquid hydrogen, ammonia, and batteries on bulk carriers, tankers, and container ships. These AMECs are selected for their future predicted presence according to Liu and Duru 2019 and additionally for their highest contained energy density for their type according to DNV-GL 2019a. For example, LNG is preferred over CNG because it requires less volume and weight, but both enter the power plant as natural gas. The selected ship types are selected because they account for 85% of the global seagoing merchant ships of +100 GT in 2021 (UNCTAD 2021). These ship types, amongst others, must comply with the GHG emissions regulation by the IMO (2015).

2.1 Constant operational requirements

To fulfil the original tasks of a ship with a new design, the following five aspects must remain constant. The first constant aspect is the ship type and accompanying design elements/trends. The new design must adhere to the historic dimension trends and contain the original elements according to Andrews and Dicks (1997). The original overall internal volume minus the fuel oil bunker volume must remain constant. It is assumed that this volume accommodates all the systems and cargo space for the payload ship function (Levander 2003). It is necessary that the service speed and sailing range/endurance remain constant to transport its cargo from port to port in the predetermined amount of time. Lastly, the non-propulsive energy consumers, such as hotel services, do not change as they are not significantly related to ship size and weight.

1. Ship type (design elements/dimension trends)
2. Original overall internal volume minus the bunker volume
3. Service speed
4. Sailing range/endurance
5. Non propulsive energy consumers (ship functioning and cargo handling/treatment)

3 Model description

The total model consists of an iterative sequence of four sub-models: parameters, resistance approximation, power approximation, and design generation. The iterative model approach is displayed in figure 2. The model starts with the original (0) ship design parameters which already fulfils all the operational requirements for its multipurpose objective. With the parameters, the original resistance is approximated using the resistance calculation sub-model. With the original resistance, the original propulsion powering is approximated in the power approximation sub-model. Thereafter the first step of the design generation model is conducted by substituting the fuel oil (1) with an AMEC, based on equal effective energy. With the first revision design, the first revision parameters, resistance and propulsion power are approximated in the sub-models. The second step of the design impact model is conducted by upscaling the AMEC bunkering (2) proportionate to the total installed engine power change ($\Delta P_{B,\,TOT}$) caused by the first revision design. As an example, see the second column of the final design and powering impact results in tables 3, 4, and 5. Once again, the second and final ship parameters, resistance and powering are determined using the sub-models.

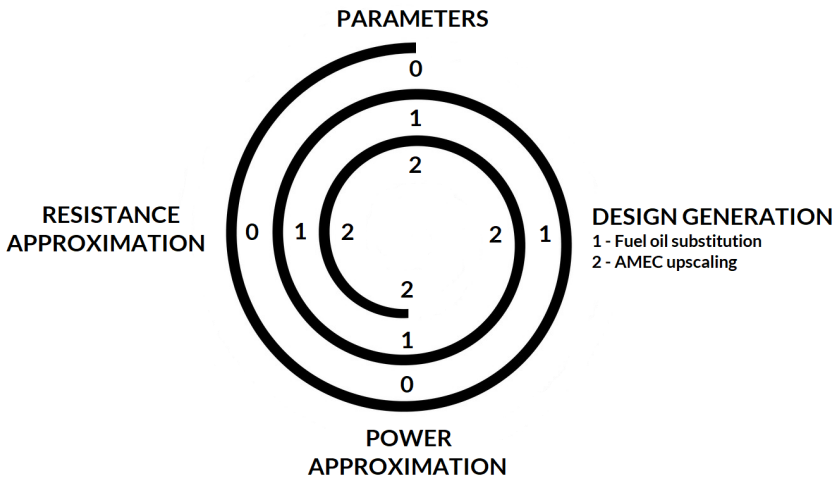

Figure 2. Iterative total model approach

3.1 Sub-model: Parameters

The parameter determination is the first sub-model, where highly detailed information of twelve ships per ship type is acquired to represent the ship type. The highly detailed information of these sampled ships are acquired from the magazine Significant Ships editions 2015 to 2020 (The Royal Institution of Naval Architects 2016) (The Royal Institution of Naval Architects 2017) (The Royal Institution of Naval Architects 2018) (The Royal Institution of Naval Architects 2019) (The Royal Institution of Naval Architects 2020) (The Royal Institution of Naval Architects 2021). All entries in the Significant Ships magazines are at least 100 m in length. The names of the sampled ships per ship type are displayed in table 6 in appendix A.

The additional parameters necessary which need to be approximated are the block coefficient (C_B), overall internal volume (V_{INT}), and the lightweight ship (m_{LIGHT}). The initial block coefficient is calculated according to the formula by Jensen 1994 according to equation 1 in which W is the Lambert function. The initial overall internal volume is calculated using the inverse formula for the calculation of the gross tonnage (GT) from the International Convention on Tonnage Measurement of Ships (IMO 1969). The lightweight ship is equal to the gravimetric displacement (Δ) minus the deadweight tonnage (DWT) and is calculated according to equation 3.

$$C_B = -4.22 + 27.8 \cdot \sqrt{F_n} - 39.1 \cdot F_n + 46.6 \cdot F_n^3 \quad [-] \tag{1}$$

$$GT = V_{INT} \cdot (0.2 + 0.02 \cdot \log_{10}(V_{INT})) \quad \rightarrow \quad V_{INT} = \frac{50 \cdot In(10) \cdot GT}{W\left(5 \cdot 10^{14} \cdot In(10) \cdot GT\right)} \quad [m^3] \tag{2}$$

$$m_{LIGHT} = \Delta - DWT = C_B \cdot L_{WL} \cdot B \cdot T \cdot \rho_{sw} - DWT \quad [t] \tag{3}$$

3.2 Sub-model: Resistance approximation

The resistance approximation sub-model is conducted according to the Holtrop & Mennen method. The method is based on a regressional statistical analysis from random model tests and full scale ship trials (Holtrop and Mennen 1982). It is considered to be efficient and accurate for determining the required propulsive power with a limited amount of ship design parameters(Nikolopoulos and Boulougouris 2019). The method is established on the basis of five papers (in chronological order) by Holtrop 1977, Holtrop and Mennen 1978, Holtrop and Mennen 1982, Holtrop 1984, and Holtrop 1988. The newer papers contain re-assessments of parts of the previous papers for higher accuracy. Therefore the compilation by Birk 2019 of the appropriate parts of the papers is used.

3.3 Sub-model: Power approximation

The propulsion power approximation sub-model is conducted according to the propulsion chain method by Klein Woud and Stapersma 2002. The required input for the propulsion approximation method consists of the sampled ship parameters and the output parameters from the resistance approximation sub-model. Additional parameters are the open water propeller efficiency (η_O), shaft efficiency (η_S), gearbox efficiency (η_{GB}), and engine margin (EM). The typical values for the efficiencies according to MAN Energy Solutions 2018 are:

η_O = 0.625 [-]
η_S = 0.990 [-]
η_{GB} = 1.000 [-] (directly coupled)
EM = 12.5 %

3.4 Sub-model: Design generation

The design generation is done twice in the total model approach. The additional contained AMEC bunker volume and weight is first calculated before each revision and thereafter applied to the original design minus the contained fuel oil bunker space. It is performed once to accommodate for the substitution of fuel oil bunker space with that of an AMEC (first revision). The second revision is performed to accommodate the upscaling of the AMEC bunker space proportionate to the propulsion power increased caused by the first revision ship design.

Lindstad et al. determined that higher length-beam ratios for ships with equal carrying capacity are the most energy efficient (Lindstad, Jullumstrø, and Sandaas 2013) (Lindstad, Sandaas, and Steen 2014). Additionally, Liu and Pananikolauo determined that the added ship resistance decreases for lower Froude numbers, which can be achieved by increasing the length of a ship (Liu and Papanikolaou 2019). For that reason, to accommodate the additional AMEC bunker space, the ship is first lengthened at the midship transverse plane area (a). Thereafter heightened at the water plane area (b) and if necessary widened in the center plane area (c). The sequence design generation sequence is depicted in figure 3. The lengthening is constrained to a maximum length-beam ratio within the length-beam ratio trend per ship type.

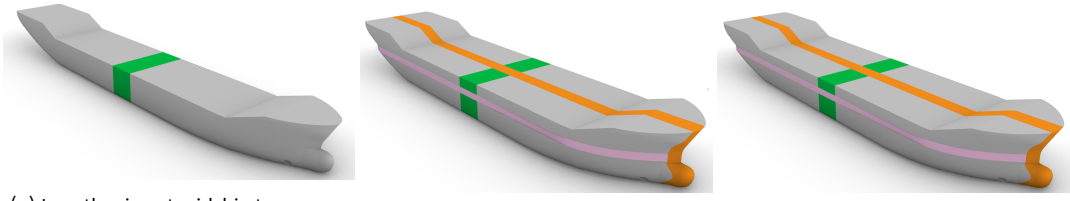

(a) Lengthening at midship transverse plane area (b) Lengthening at water plane area (c) Widened at center plane area

In the following subsections, the method of calculating the additional AMEC bunker space is elaborated for the fuel oil substitution and the upscaling of the AMEC bunker volume respectively. Thereafter, the procedure of applying the calculated additional AMEC bunker space from the previous subsections is explained.

Figure 3. The design generation sequence to accommodate additional AMEC bunker space

Design trends and spatial aspects

The length-beam ratio trends per ship type is constructed using the World Fleet Register by Clarksons Research (2022). The Clarksons data is filtered for ships ≥ 100 meters in length and built between 2015 and 2020 to coincide with the Significant Ships entry conditions. The length-beam ratios of the Clarksons ships and Significant Ships data are displayed in figures 4, 5, and 6 for bulk carriers, tankers and container ships respectively. The maximum length-beam ratio constraint formula per ship type is displayed in equation 4 and the parameters per ship type are displayed in table 1. The linear equation parameters are selected to intersect the highest length-beam ratio of a highly dense coordinate (dark blue) at higher ship lengths. The slope is adjusted in order for the highest length-beam ratios of a highly dense coordinates at lower ship lengths to be beneath than the line. This approach is chosen as it is expected that ships with higher lengths are less capable of being lengthened further compared to widening.

$$L_{OA}/B_{MAX,\,ship\,type} = a \cdot L_{OA} + b \quad [-] \tag{4}$$

Table 1. Maximum length-beam ratio constraint parameters

Ship type	*a*	*b*
Bulk carriers	-0.0125858	10.1251
Tankers	-0.0080163	8.3795
Container ships	0.0047341	5.8620

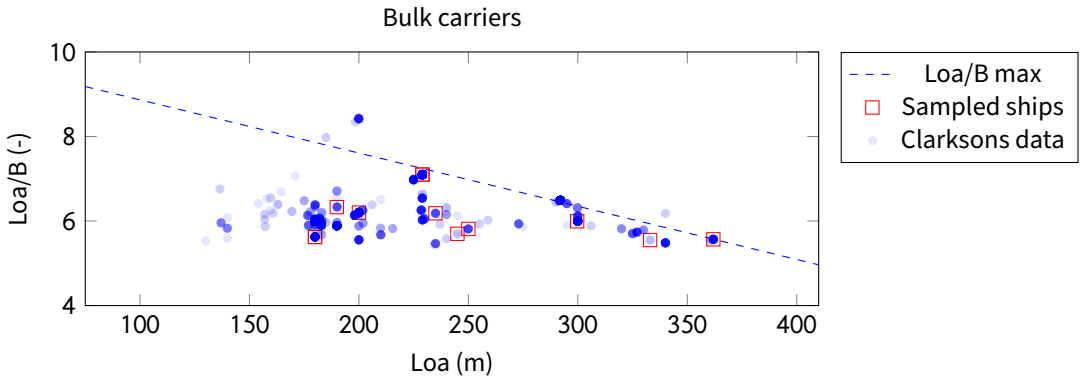

Figure 4. Length-beam ratio of Clarksons data and sampled bulk carriers

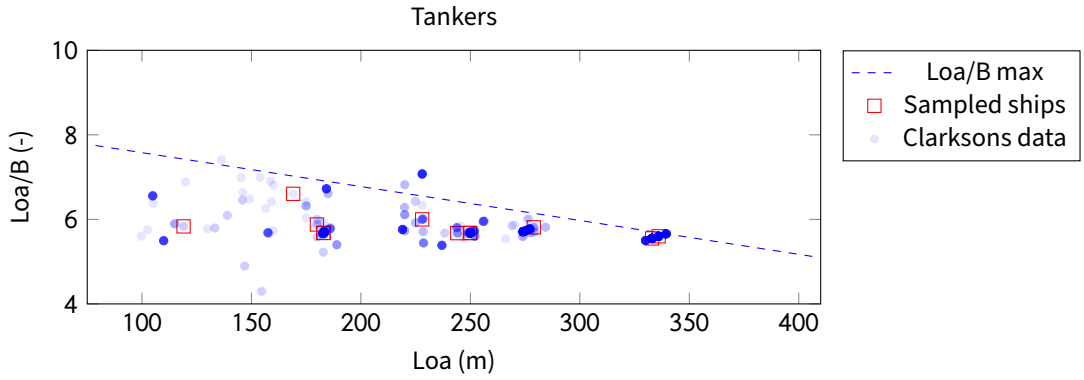

Figure 5. Length-beam ratio of Clarksons data and sampled tankers

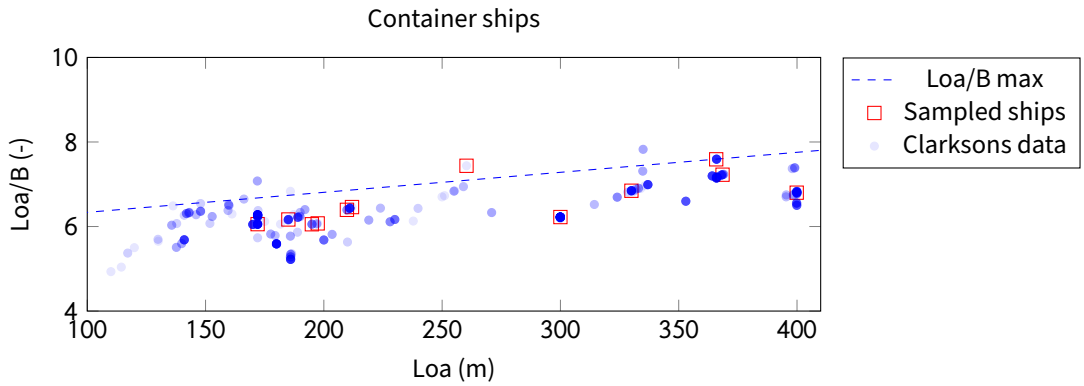

Figure 6. Length-beam ratio of Clarksons data and sampled container ships

The necessary AMEC bunker volume and weight is determined using the contained volumetric and gravimetric energy density ($\rho_{V\ E\ con}$ and $\rho_{G\ E\ con}$), total power plant efficiency η_{PP}, and auxiliary power necessary for the power plant to function as a percentage of the main engine power (PP_{aux}). The values are displayed in table 2. The auxiliary power necessary for the power plant to function ($P_{B,\ AE\ PP}$) is the power for the equipment for the energy carrier handling. For example, pumps, filters, heating elements, coolers, etc. This parameter demonstrates that for fuel cell power plants, an additional installed power of 6% is necessary, whereas for batteries it is 4% less.

Table 2. Overview power plant efficiencies and energy densities of (A)MEC types

	Power plant		Contained			Uncontained		
	η_{PP}	PP_{aux}	$\rho_{V\ E\ con}$	$\rho_{G\ E\ con}$	ρ_{con}	$\rho_{V\ E\ uncon}$	$\rho_{G\ E\ uncon}$	ρ_{uncon}
	-	-	MJ/L	MJ/kg	kg/L	MJ/L	MJ/kg	kg/L
Fuel oil (original)	49.3%	5%	33.20	29.65	1.12	35.70	41.00	0.87
Methanol	49.3%	3%	13.83	15.67	0.88	15.60	19.90	0.78
LNG	48.6%	3%	13.37	28.38	0.47	22.37	49.20	0.45
Liq. hydrogen [a]	43.9%	11%	4.60	11.70	0.39	7.55	120.00	0.06
Ammonia [a]	51.3%	11%	9.45	11.70	0.81	12.70	22.00	0.58
Batteries	85.7%	1%	0.22	0.33	0.67	2.98	0.50	5.96

[a] Fuel cell power plant

Energy densities inspired by DNV-GL (2019a), Vuyk Engineering (2021), Biert *et al.* (2016)

Design generation: fuel oil substitution

The design generation for the fuel oil substitution is performed by calculating the necessary AMEC bunker space requirements for equal effective energy. The total effective energy ($E_{eff,\,total}$) of the bunkered fuel oil on board is calculated with the original fuel oil bunker volume ($V_{BUNK,\,FO}$) and the values from table 2. The total effective energy is calculated according to equation 5.

$$E_{eff,\,total} = V_{BUNK,\,FO} \cdot \rho_{V\,E,\,FO\,con} \cdot \eta_{PP,\,FO} \quad [MJ] \tag{5}$$

The total effective energy is divided based on the consumers: the main engine(s) ($E_{eff,\,ME}$) and the auxiliary engine(s) ($E_{eff,\,AE}$) according to equation 6. The main engine effective energy and auxiliary engine effective energy division is determined based on the specific fuel consumption (sfc) and brake power (P_B). A specific fuel consumption of 170 g/kWh is selected for a two stoke diesel engine and 207.5 g/kWh for a four stroke diesel engine (Lamb 2003). The main engine effective energy and auxiliary engine effective energy are calculated according to equation 7 and 8 respectively.

$$E_{eff,\,total} = E_{eff,\,ME} + E_{eff,\,AE} \quad [MJ] \tag{6}$$

$$E_{eff,\,ME} = \frac{sfc_{ME} \cdot P_{B,\,ME}}{sfc_{ME} \cdot P_{B,\,ME} + sfc_{AE} \cdot P_{B,\,AE}} \cdot E_{eff,\,total} \quad [MJ] \tag{7}$$

$$E_{eff,\,AE} = E_{eff,\,total} - E_{eff,\,ME} \quad [MJ] \tag{8}$$

The auxiliary engine effective energy is split into power plant users ($E_{eff,\,AE\,PP}$) and non-power plant users ($E_{eff,\,AE\,non-PP}$) according to equation 9. The auxiliary engine effective energy for the power plant users ($E_{eff,\,AE\,PP}$) is calculated with the auxiliary power necessary for the power plant to function as a percentage of the main engine power (PP_{aux}) according to equation 10. The remaining auxiliary engine effective energy for non-power plant users ($E_{eff,\,AE\,non-PP}$) is calculated according to equation 11.

$$E_{eff,\,AE} = E_{eff,\,AE\,PP} + E_{eff,\,AE\,non-PP} \quad [MJ] \tag{9}$$

$$E_{eff,\,AE\,PP} = \frac{PP_{aux,\,FO} \cdot P_{B,\,ME}}{P_{B,\,AE}} \cdot E_{eff,\,AE} \quad [MJ] \tag{10}$$

$$E_{eff,\,AE\,non-PP} = E_{eff,\,AE} - E_{eff,\,AE\,PP} \quad [MJ] \tag{11}$$

The total effective energy for an AMEC is calculated according to equation 12. It is slightly different due to the auxiliary power necessary for the power plant to function as a percentage of the main engine power (PP_{aux}).

$$E_{eff,\,total\,AMEC} = E_{eff,\,ME} + E_{eff,\,AE\,PP} \cdot \frac{PP_{aux,\,AMEC}}{PP_{aux,\,FO}} + E_{eff,\,AE\,non-PP} \quad [MJ] \tag{12}$$

The resulting total bunker volume by an AMEC ($V_{BUNK,\,AMEC}$) is calculated according to equation 13 and the total bunker weight by an AMEC ($m_{BUNK,\,AMEC}$) is calculated according to equation 14. The original fuel oil bunker volume and weight are subtracted from the necessary total AMEC bunker volume and weight, yielding the additional AMEC bunker volume ($\Delta V_{BUNK,\,AMEC}$) and weight ($\Delta m_{BUNK,\,AMEC}$) according to equation 15 and 16 respectively.

$$V_{BUNK,\,AMEC} = \frac{E_{eff,\,total\,AMEC}}{\rho_{V\,E\,con\,AMEC} \cdot \eta_{PP\,AMEC}} \quad [L] \tag{13}$$

$$m_{BUNK,\,AMEC} = V_{BUNK,\,AMEC} \cdot \rho_{con\,AMEC} \quad [kg] \tag{14}$$

$$\Delta V_{BUNK,\,AMEC} = \left(V_{BUNK,\,AMEC} - V_{BUNK,\,FO}\right) \cdot 1000 \quad [m^3] \tag{15}$$

$$\Delta m_{BUNK,\,AMEC} = \left(m_{BUNK,\,AMEC} - m_{BUNK,\,FO}\right) \cdot 1000 \quad [t] \tag{16}$$

Additional AMEC bunker space application procedure

The maximum length overall for a ship ($L_{OA,\,MAX}$) is calculated according to equation 19, using the mathematical maximum length-beam ratio constraint formula per ship type formula in equation 17 and the mathematical current length-beam ratio formula in equation 18. The maximum additional length (ΔL_{MAX}) and consequently the maximum volume available by lengthening the ship ($\Delta V_{L,\,MAX}$) are calculated according to equations 20 and 21 respectively.

$$L_{OA}/B_{MAX,\,ship\,type} \quad = \quad a \cdot L_{OA} + b \quad = \quad a \cdot x + b \quad [-] \tag{17}$$

$$L_{OA}/B_{ship} \quad = \quad \frac{1}{B} \cdot L_{OA} \quad = \quad c \cdot x \quad [-] \tag{18}$$

$$a \cdot x + b = c \cdot x \quad \rightarrow \quad x = \frac{b}{c - a} = \frac{b}{\frac{1}{B} - a} = L_{OA,\,MAX} \quad [m] \tag{19}$$

$$\Delta L_{MAX} = L_{OA,\,MAX} - L_{OA} \quad [m] \tag{20}$$

$$\Delta V_{L,\,MAX} = A_{MID} \cdot \Delta L_{MAX} \quad [m^3] \tag{21}$$

The actual lengthening (ΔL) is calculated according to equation 22 if the necessary additional AMEC bunker volume is less than the maximum volume available by lengthening. Only 50% of the necessary additional AMEC bunker volume is applied, because the heightening in the next step is done for constant depth-length ratio. Therefore, the additional volume by heightening is practically the same volume. The actual lengthening, in the condition that the necessary additional AMEC bunker volume exceeds the maximum volume available by lengthening, is calculated according to equation 23. Accordingly, the actual additional volume by lengthening (ΔV_L) is calculated according to equation 24. The remaining volume after lengthening ($\Delta V_{BUNK,\,REMAIN\,L}$) is calculated according to equation 25.

$$\Delta L \quad (\Delta V_{BUNK,\,AMEC} < \Delta V_{L,\,MAX}) = \frac{50\% \cdot \Delta V_{BUNK,\,AMEC}}{A_{MID}} \quad [m] \tag{22}$$

$$\Delta L \quad (\Delta V_{BUNK,\,AMEC} > \Delta V_{L,\,MAX}) = \Delta L_{MAX} \quad [m] \tag{23}$$

$$\Delta V_L = \Delta L \cdot A_{MID} \quad [m^3] \tag{24}$$

$$\Delta V_{BUNK,\,REMAIN\,L} = \Delta V_{BUNK,\,AMEC} - \Delta V_L \quad [m^3] \tag{25}$$

The heightening (ΔD) is calculated by keeping the original depth-length ratio constant according to equation 26. Accordingly, the additional volume by heightening is calculated according to equation 27 with the new water plane area ($A_{WP,\,new}$). The remaining volume after heightening ($\Delta V_{BUNK,\,REMAIN,\,D}$) is calculated according to equation 28.

$$\Delta D = \frac{D_{original}}{L_{OA,\,original}} \cdot \Delta L \quad [m] \tag{26}$$

$$\Delta V_D \quad = \quad \Delta D \cdot A_{WP,\,new} \quad [m^3] \tag{27}$$

$$\Delta V_{BUNK,\,REMAIN,\,D} = \Delta V_{BUNK,\,REMAIN\,L} - \Delta V_D \quad [m^3] \tag{28}$$

There are three scenarios for calculating the additional volume by widening (ΔV_B) according to equation 29. The first is if there is a positive remaining volume after heightening ($\Delta V_{BUNK,\,REMAIN,\,D}$). In general this is always the case unless the waterplane area coefficient is larger than the midship area coefficient ($C_{WP} > C_M$). The second scenario is for when the remaining volume after heightening is negative. In this case, there is more volume applied to the ship design than required and therefore the excess volume is considered a surplus volume ($\Delta V_{SURPLUS}$) and calculated according to equation 30. Consequently, the additional volume by widening is zero and the surplus volume is deducted from the necessary AMEC bunker volume for the second revision design generation (AMEC upscaling) later on in equation 44. The third scenario is if the original length-beam ratio exceeds the maximum length-beam ratio line ($L/B > L/B_{MAX}$). In this case, the lengthening and heightening is skipped and the total additional AMEC bunker volume is immediately applied by widening. The resulting widening is calculated according to equation 31.

$$\begin{aligned} \Delta V_B \quad (\Delta V_{BUNK,\,REMAIN,\,D} > 0) &= \Delta V_{BUNK,\,REMAIN,\,D} \quad [m^3] \\ \Delta V_B \quad (\Delta V_{BUNK,\,REMAIN,\,D} < 0) &= 0 \quad [m^3] \\ \Delta V_B \quad (L/B_{original} > L/B_{MAX}) &= \Delta V_{BUNK,\,AMEC} \quad [m^3] \end{aligned} \tag{29}$$

$$\begin{aligned} \Delta V_{SURPLUS} \quad (\Delta V_{BUNK,\,REMAIN,\,D} > 0) &= 0 \quad [m^3] \\ \Delta V_{SURPLUS} \quad (\Delta V_{BUNK,\,REMAIN,\,D} < 0) &= -\Delta V_{BUNK,\,REMAIN,\,D} \quad [m^3] \end{aligned} \tag{30}$$

$$\Delta B = \frac{\Delta V_B}{A_{CP,\,new}} \quad [m] \tag{31}$$

New ship parameter determination

The sub-model formulas in section 3.1 approximate the original parameters. In this subsection, the new parameters are determined. The new main dimensions (L_{new}, D_{new}, andB_{new}) are calculated according to equations 32, 33, and 34 respectively. The new draft (T_{new}) is calculated according to equation 35, where the additional AMEC bunker weight ($\Delta m_{BUNK,\,AMEC}$) and the structural weight of steel (W_S) are accounted for. According to Friis, Anderson, and Jensen 2002, the typical steel structure density for ships > 10.000 t is 0.08 t/m^3. The new propeller diameter ($D_{P,\,new}$) is increased proportionately to the draft increase according to equation 36.

$$L_{new} = L + \Delta L \quad [m] \tag{32}$$

$$D_{new} = D + \Delta D \quad [m] \tag{33}$$

$$B_{new} = B + \Delta B \quad [m] \tag{34}$$

$$\begin{aligned} T_{new} &= T + \Delta T \quad [m] \\ &= T + \frac{\Delta m_{BUNK,\,AMEC} + W_S}{A_{WP,\,new} \cdot \rho_{sw}} \quad [m] \\ &= T + \frac{\Delta m_{BUNK,\,AMEC} + C_S \cdot (\Delta V_L + \Delta V_D + \Delta V_B)}{A_{WP,\,new} \cdot \rho_{sw}} \quad [m] \end{aligned} \tag{35}$$

$$D_{P,\,new} = \frac{T_{new}}{T} \cdot D_P \quad [m] \tag{36}$$

The new overall internal volume ($V_{INT,\,new}$) is calculated by summing the additional volumes by lengthening, heightening and widening according to equation 37. The new deadweight tonnage (DWT_{new}) is calculated according to equation 38 for the depleting AMECs. The new deadweight tonnage specifically for the full electric battery configuration is calculated according to equation 39. The new lightweight ship ($m_{LIGHT\ new}$) is calculated according to equation 40.

$$V_{INT,\,new} = V_{INT} + \Delta V_L + \Delta V_D + \Delta V_B \quad [m^3] \tag{37}$$

$$DWT_{new} = DWT - m_{FO\ uncon} + m_{AMEC\ uncon} \quad [t] \tag{38}$$

$$DWT_{new\ BATTERY} = DWT - m_{FO\ uncon} \quad [t] \tag{39}$$

$$m_{LIGHT,\,new} = \Delta_{new} - DWT_{new} \quad [t] \tag{40}$$

The total installed engine brake power ($P_{B,\,TOT}$) is calculated according to equation 41. The auxiliary engine brake power for the non-power plant consumers ($P_{B\ AE\ non-PP}$) remains constant and the auxiliary engine brake power for the power plant consumers ($P_{B\ AE\ PP}$) is a percentage of the main engine brake power ($P_{B\ ME}$).

$$\begin{aligned} P_{B,\,TOT} &= P_{B\ ME} + P_{B\ AE} \quad [kW] \\ &= P_{B\ ME} + P_{B\ AE\ PP} + P_{B\ AE\ non-PP} \quad [kW] \\ &= P_{B\ ME} \cdot (1 + PP_{aux}) + P_{B\ AE\ non-PP} \quad [kW] \end{aligned} \tag{41}$$

Design generation: AMEC upscaling

The design generation for upscaling the AMEC bunker space is performed by scaling the AMEC bunker space requirements proportionately to the main engine power increase. The additional AMEC total effective energy ($\Delta E_{eff,\,total\ AMEC}$) is calculated according to equation 42, where the main engine power increase ($P_{B,\,ME\ AMEC\ 1}/P_{B,\,ME\ FO}$) is the result from the first revision power approximation. The gross additional AMEC bunker volume ($\Delta V_{BUNK,\,AMEC\ GROSS}$) is calculated is calculated according to equation 43. As mentioned previously, the AMEC bunker space application procedure can result in a minor surplus internal volume and therefore it is deducted from the gross volume according to equation 44, yielding the net additional AMEC bunker volume ($\Delta V_{BUNK,\,AMEC}$). The resulting additional AMEC bunker weight ($\Delta m_{BUNK,\,AMEC}$) is calculated according to equation 45.

$$\Delta E_{eff,\,total\ AMEC} = \left(\frac{P_{B,\,ME\ AMEC\ 1}}{P_{B,\,ME\ FO}} - 1\right) \cdot \left(E_{eff,\,total\ AMEC} - E_{eff,\,AE\ non-PP}\right) \quad [MJ] \tag{42}$$

$$\Delta V_{BUNK,\,AMEC\ GROSS} = \frac{\Delta E_{eff,\,total\ AMEC}}{\rho_{V\ E\ con\ AMEC} \cdot \eta_{PP\ AMEC} \cdot 1000} \quad [m^3] \tag{43}$$

$$\Delta V_{BUNK,\,AMEC} = \Delta V_{BUNK,\,AMEC\ GROSS} - \Delta V_{SURPLUS} \quad [m^3] \tag{44}$$

$$\Delta m_{BUNK,\,AMEC} = \Delta V_{BUNK,\,AMEC} \cdot \rho_{con\ AMEC} \quad [t] \tag{45}$$

4 Results

The results for the total installed power change ($\Delta P_{B,\,TOT}$), main engine brake power change ($\Delta P_{B,\,ME}$), overall internal volume change (ΔV_{INT}), lightweight ship change (Δm_{LIGHT}), deadweight tonnage change (ΔDWT), and length-beam ratio change ($\Delta L/B$) are displayed in table 3, 4, and 5 for bulk carriers, tankers, and container ships respectively.

Table 3. Design and powering impact results for bulk carriers w.r.t. fuel oil

AMEC	$\Delta P_{B,\,TOT}$	$\Delta P_{B,\,ME}$	ΔV_{INT}	Δm_{LIGHT}	ΔDWT	$\Delta L/B$
Methanol	+1.9%	+2.3%	+2.7%	+4.1%	+2.4%	+0.8%
LNG	+0.9%	+1.1%	+2.9%	+5.1%	-0.4%	+0.9%
Liq. hydrogen	+8.6%	+10.3%	+18.1%	+62.7%	-1.2%	+2.2%
Ammonia	+3.7%	+4.4%	+5.3%	+21.8%	+2.2%	+1.0%
Batteries	+235.3%	+280.8%	+509.9%	+2514.0%	-2.3%	-15.8%

Table 4. Design and powering impact results for tankers w.r.t. fuel oil

AMEC	$\Delta P_{B,\,TOT}$	$\Delta P_{B,\,ME}$	ΔV_{INT}	Δm_{LIGHT}	ΔDWT	$\Delta L/B$
Methanol	+1.6%	+2.2%	+2.7%	+1.8%	+2.8%	+1.0%
LNG	+0.8%	+1.1%	+2.8%	+2.3%	-0.4%	+1.1%
Liq. hydrogen	+7.4%	+9.8%	+17.6%	+27.6%	-1.5%	+5.3%
Ammonia	+3.2%	+4.2%	+5.2%	+9.6%	+2.5%	+1.9%
Batteries	+234.4%	+309.7%	+552.0%	+1118.1%	-2.6%	-14.5%

Table 5. Design and powering impact results for container ships w.r.t. fuel oil

AMEC	$\Delta P_{B,\,TOT}$	$\Delta P_{B,\,ME}$	ΔV_{INT}	Δm_{LIGHT}	ΔDWT	$\Delta L/B$
Methanol	+2.6%	+3.1%	+3.8%	+3.5%	+6.0%	+1.2%
LNG	+1.0%	+1.2%	+4.0%	+4.3%	-0.9%	+1.3%
Liq. hydrogen	+8.4%	+10.2%	+22.3%	+51.1%	-3.1%	+7.8%
Ammonia	+4.9%	+5.9%	+7.4%	+18.5%	+5.5%	+2.4%
Batteries	+190.1%	+229.7%	+490.5%	+1881.7%	-5.6%	+127.1%

5 Discussion

The constant operational requirements have been investigated under the condition that the main ship dimensions are not a part of it. However, traditionally ships are designed to maximize its dimensions to the spatial limits of locks, canals, bridges, etc. Therefore, it is possible that the newly generated ship designs exceed the spatial limitations and consequently it cannot perform its operational tasks.

In general the length-beam ratios of the new ship designs increase for all AMEC type and ship type combination. Ships with an original length-beam ratio right beneath the maximum length-beam ratio line marginally decrease in length-beam ratio. The length-beam ratio for the single container ship above the maximum length-beam ratio line has the highest length-beam ratio decrease. In general the new length-beam ratios of container ships are higher than bulk carriers and tankers due to the positive slope (a) in the maximum length-beam ratio formula.

The calculated additional AMEC bunker space includes the storage tank and necessary handling systems, but it was applied in the design procedure as if it was one fluid volume. Therefore the design procedure does not distinguish between storage tank and handling systems as separate locations in the ship. Accordingly, the location requirements of storage tanks and handling systems were not taken into account. However it is assumed that the general arrangement can be reconstructed with the new design to adhere to the location requirements.

The additional AMEC bunker space application procedure does not take redundant overall internal volume into account in the original design. Therefore, it is possible that the overall internal volume change can be reduced by taking this factor into account. For example, double bottoms containing ballast water are likely unnecessary for batteries due to the weight. Moreover, batteries in all ship types require at least an additional five times the original volume. As a result, these ship designs are impractically large compared to other AMECs. Consequently, the length-beam ratios of battery powered bulk carriers and tankers decrease due to the high volume application.

Similar to the overall internal volume change, the lightweight ship increases for all AMEC-ship type combinations. The additional lightweight ship for batteries in all ship types is significantly high with a minimum average of +1118% in tankers. As a result, of the twelve ships per ship type, eight bulk carriers and two tankers do not even float with their newly generated design. Moreover, the utilization rate of the DWT in relation to the ship's weight is considerably low for battery powered ships compared to other AMECs.

Lastly, the design procedure is optimized for the least amount of additional resistance which is calculated with the Holtrop & Mennen method. The resistance approximation method is around 35 years old and ship designs have become more energy efficient in the mean time. Accordingly, the resistance results can be interpreted as less accurate. Especially when considering that the sampled ships originate from the magazine Significant Ships and in various cases their energy efficient design makes them 'significant'.

Furthermore, the additional AMEC bunker space application procedure is performed on existing ship designs. Therefore, the procedure does not necessarily represent the actual ship designing procedure for newly built ships. The design procedure optimizes for the least amount of additional resistance for a new design based on an existing smaller design. A ship design has a multipurpose objective to perform all of its tasks and therefore following the lengthening, heightening, widening sequence might not result in the optimal design as a new build.

6 Conclusion

A model has been developed to determine a new design and powering impact for existing ships with the predicted marine energy carriers of the future. The results indicate that for constant operational requirements, bulk carriers, tankers and container ships will become larger and heavier for all future energy carriers. As expected, a larger and heavier ship requires a higher main engine power and therefore a higher total installed power as well. The total installed power increase in bulk carriers, tankers and container ships is 3-5% for methanol, LNG, and ammonia; 7-9% for liquid hydrogen; and 190-235% for batteries.

The total installed power increase results are intended to support a research on the total environmental impact. The total installed power increase is proportionate to the energy carrier consumption increase and therefore must be taken into account as well. The current greenhouse gas emissions regulations target direct CO_2 emissions, yet the emissions caused by the production and distribution are not taken into account. It is possible that the use of alternative marine energy carriers with current ship designs are more environmentally friendly. However, it has not been researched if this is still the case when taking the increased energy carrier consumption into account due to the design and powering impact for constant operational requirements.

References

Andrews, D., and C. Dicks. 1997. "The building block design methodology applied to advanced naval ship design."

Biert, L. van, M. Godjevac, K. Visser, and P. Aravind. 2016. "A review of fuel cell systems for maritime applications." *Journal of Power Sources* 327:345–364.

Birk, L. 2019. *Holtrop and Mennen's Method.* 611–627. John Wiley & Sons, Ltd, April. ISBN: 9781118855485. https://doi.org/10.1002/9781119191575.ch50. https://onlinelibrary.wiley.com/doi/10.1002/9781119191575.ch50.

Bodewes, W. 2020. "A conceptual design study to prepare a general cargo ship for a refit towards alternative fuels." Master's thesis, Delft University of Technology.

Bureau Veritas. 2021. *EEXI and CII: Dual regulations reducing ship's carbon impact.* May.

Clarksons Research. 2022. *World fleet register.*

DNV-GL. 2019a. *Comparison of Alternative Marine Fuels.* July.

———. 2019b. *Maritime Forecast To 2050: Energy Transition Outlook 2019.*

Friis, A., P. Anderson, and J. Jensen. 2002. "Ship design (Part 1 & II)." *Section of Maritime Engineering, Dept. of Mechanical Engineering, Technical University of Denmark, Denmark.*

Holtrop, J. 1977. "Statistical analysis of performance test results." *International Shipbuilding Progress* 24 (270).

———. 1984. "A statistical re-analysis of resistance and propulsion data." *International Shipbuilding Progress* 28 (363): 272.

———. 1988. "A statistical resistance prediction method with a speed dependent form factor." *Proceedings of the 17th Session BSHC, Varna* 1:3–1.

Holtrop, J., and G. Mennen. 1978. "A statistical power prediction method." *International shipbuilding progress* 25 (290).

———. 1982. "An approximate power prediction method." *International Shipbuilding Progress* 29 (335): 166–170.

IMO. 1969. *International Convention on Tonnage Measurement of Ships.*

IMO. 2015. “TTT course on energy efficient ship operation – M2 ship energy efficiency regulations and related guidelines.”

IPCC. 2021. *Climate Change 2022: Mitigation of Climate Change. Contribution of Working Group III to the Sixth Assessment Report of the Intergovernmental Panel on Climate Change.*

Jensen, G. 1994. “Moderne Schiffslinien.” *Handbuch der Werften* XXII.

Klein Woud, J., and D. Stapersma. 2002. *Design of Propulsion and Electric Power Generation Systems.* 64. IMarEST.

Lamb, T. 2003. *Ship Design and Construction.* SNAME. ISBN: 0-939773-40-6.

Levander, K. 2003. “Innovative Ship Design–Can innovative ships be designed in a methodological way.” In *Proc. 8th Int. Marine Design Conference–IMDC03, Athens.*

Lindstad, H., E. Jullumstrø, and I. Sandaas. 2013. “Reductions in cost and greenhouse gas emissions with new bulk ship designs enabled by the Panama Canal expansion.” *Energy Policy* 59:341–349.

Lindstad, H., I. Sandaas, and S. Steen. 2014. “Assessment of profit, cost, and emissions for slender bulk vessel designs.” *Transportation Research Part D: Transport and Environment* 29:32–39.

Liu, J., and O. Duru. 2019. “Future of marine fuel: Five projections of marine fuels from 2020 to 2050.” *Okan Duru, Shipping Economics and Research.*

Liu, S., and A. Papanikolaou. 2019. “Approximation of the added resistance of ships with small draft or in ballast condition by empirical formula.” *Proceedings of the Institution of Mechanical Engineers, Part M: Journal of Engineering for the Maritime Environment* 233 (1): 27–40.

MAN Energy Solutions. 2018. *Basic principles of ship propulsion.*

Nikolopoulos, L., and E. Boulougouris. 2019. “A Study on the Statistical Calibration of the Holtrop and Mennen Approximate Power Prediction Method for Full Hull Form, Low Froude Number Vessels.” *Journal of Ship Production and Design* 35 (01): 41–68. ISSN: 2158-2866. https://doi.org/10.5957/JSPD.170034. https://onepetro.org/JSPD/article/35/01/41/173670/A-Study-on-the-Statistical-Calibration-of-the.

Terün, K., A. A. Kana, and R. Dekker. 2022. “Assessing Alternative Fuel Types for Ultra Large Container Vessels in Face of Uncertainty.” In *21st Conference on Computer and IT Applications in the Maritime Industries (COMPIT’22).*

The Royal Institution of Naval Architects. 2016. *Significant Ships of 2015.*

———. 2017. *Significant Ships of 2016.*

———. 2018. *Significant Ships of 2017.*

———. 2019. *Significant Ships of 2018.*

———. 2020. *Significant Ships of 2019.*

———. 2021. *Significant Ships of 2020.*

UNCTAD. 2021. *Review of Maritime Transport 2021.* United Nations, December. ISBN: 9789210000970. https://doi.org/10.18356/9789210000970. https://www.un-ilibrary.org/content/books/9789210000970.

Vergragt, P. J., N. Markusson, and H. Karlsson. 2011. “Carbon capture and storage, bio-energy with carbon capture and storage, and the escape from the fossil-fuel lock-in.” *Global Environmental Change* 21 (2): 282–292.

Vuyk Engineering. 2021. “Pugh Matrix - Energy Sources” (December).

A Sampled ships

Table 6. Sampled ships per ship type

Bulk carriers		Tankers		Container ships	
Name	IMO	Name	IMO	Name	IMO
CIELO D'ITALIA	9539274	ASPHALT SPLENDOR	9763332	AL MURABBA	9708837
TRUE LOVE	9697143	D&K ABDUL RAZZAK KHALID ZAID	9700213	CMA CGM ARKANSAS	9722651
VENTURE GOAL	9670731	KMARIN RESPECT	9683001	CAPE AKRITAS	9706190
RB JORDANA	9730816	HERON	9730086	MAERSK BERMUDA	9697014
GREAT INTELLIGENCE	9800623	WHITE STAR	9799109	EVER BLISS	9786932
YUAN HE HAI	9806873	CABO VICTORIA	9778674	OOCL HONG KONG	9776171
SAO DIANA	9822255	IBERIAN SEA	9815604	DANIEL K INOUYE	9719056
ADMIRAL SCHMIDT	9838838	NAUTICAL DEBORAH	9794836	SABRE TRADER	9817884
CHINA STEEL LIBERTY	9832975	HILI	9851830	MSC JOSSELINE	9842061
DIETRICH OLDENDORFF	9860350	BOW ORION	9818515	SEATRADE GREEN	9810915
SARA	9837119	SOLAR SHARNA	9877614	KMTC SEOUL	9882205
BEATE OLDENDORFF	9853022	TOVE KNUTSEN	9868376	YM CELEBRITY	9864502